A Si/CdTe Semiconductor Compton Camera

Shin Watanabe, Takaaki Tanaka, Kazuhiro Nakazawa, Takefumi Mitani, Kousuke Oonuki, Tadayuki Takahashi, Takeshi Takashima, Hiroyasu Tajima, Yasushi Fukazawa, Masaharu Nomachi, Shin Kubo, Mitsunobu Onishi and Yoshikatsu Kuroda

***Abstract*— We are developing a Compton camera based on Si and CdTe semiconductor imaging devices with high energy resolution. In this paper, results from the most recent prototype are reported. The Compton camera consists of six layered double-sided Si Strip detectors and CdTe pixel detectors, which are read out with low noise analog ASICs, VA32TAs. We obtained Compton reconstructed images and spectra of line gamma-rays from 122 keV to 662 keV. The energy resolution is 9.1 keV and 14 keV at 356 keV and 511 keV, respectively.**

***Index Terms*— Compton Camera, Silicon radiation detectors, CdTe, Gamma-ray spectroscopy detectors, Gamma-ray astronomy detectors**

I. Introduction

THE Compton camera is the most promising approach for gamma-ray detection ranging from several tens keV to several MeV, especially in high energy astrophysics. In a Compton camera, the deposited energy and position of the gamma-ray interactions with the detector are obtained. When a gamma-ray photon is scattered in one detector and absorbed in another detector, the incident energy of the gamma-ray and the scattering angle can be determined as,

$$E_{\rm in} = E_1 + E_2 \quad (1)$$

$$\cos\theta = 1 - \frac{m_e c^2}{E_2} + \frac{m_e c^2}{E_1 + E_2}, \quad (2)$$

where E_1 is the energy of the recoil electron, E_2 is the energy of the scattered photon and θ is the scattering angle.

As shown in eq. (2), the incident direction of a gamma-ray is calculated from the position and energy information of the interactions. Therefore, employing imaging spectrometers as components of Compton cameras, with their good energy and position resolution, will dramatically improve the angular resolution and hence the sensitivity. From this point of view, Compton cameras based on semiconductors, such as Si, Ge, CZT and CdTe, have been proposed and developments are ongoing in many groups [1]–[7]. A Compton camera also enables us to measure polarization of gamma-rays, through obtaining the azimuthal distribution of Compton scattering [8], [9].

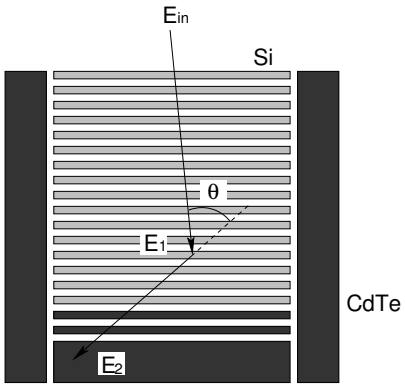

Fig. 1. Schematic picture of our Si/CdTe semiconductor Compton camera.

Based on our developments for CdTe and Si detectors [10]–[14], we have proposed a new Si/CdTe semiconductor Compton camera. Fig. 1 shows the basic concept of the Si/CdTe Compton camera. Si detectors are used as scatterers, and CdTe detectors are used as absorbers. The combination of Si and CdTe is suitable for detection of gamma-rays from several tens keV to a few MeV. The photo-absorption cross section of Si is small, and the Compton cross section becomes relatively large because of the small atomic number of Si (Z = 14). Additionally, Si works better than other materials with larger atomic numbers in terms of the "Doppler broadening" effect [15]. On the other hand, CdTe has high photo absorption efficiency for gamma-rays of this energy region, due to their high atomic numbers of 48 and 52.

We have been developing prototypes composed of double-sided Si strip detectors (DSSDs) and CdTe pixel detectors. With the first prototype consisting of one DSSD and two CdTe pixel detectors, we have obtained Compton reconstructed images and spectra from 80 keV to 356 keV [16], and have demonstrated the ability to detect polarized gamma-rays [17]. In this paper, we report the results from our second prototype of the Si/CdTe Compton camera. The prototype consists of six layered DSSDs and three 8 $\times$ 8 CdTe pixel detectors.

S. Watanabe, K. Nakazawa and T. Takashima are with Institute of Space and Astronautical Science, Japan Aerospace Exploration Agency, Sagamihara, Kanagawa, Japan.

T. Tanaka, T. Mitani, K. Oonuki and T. Takahashi are with Institute of Space and Astronautical Science, Japan Aerospace Exploration Agency, and also with Department of Physics, University of Tokyo, Bunkyo, Tokyo, Japan.

H. Tajima is with Stanford Linear Accelerator Center, Menlo Park, CA, USA.

Y. Fukazawa is with Department of Physics, Hiroshima University, Higashi Hiroshima, Hiroshima, Japan.

M. Nomachi is with Laboratory of Nuclear Studies, Osaka University, Toyonaka, Osaka, Japan.

S Kubo is with Clear Pulse Ltd., Ohta, Tokyo, Japan.

M. Onishi and Y. Kuroda are with Nagoya Guidance and Propulsion System Works, Mitsubishi Heavy Industries, Ltd., Komaki, Aichi, Japan

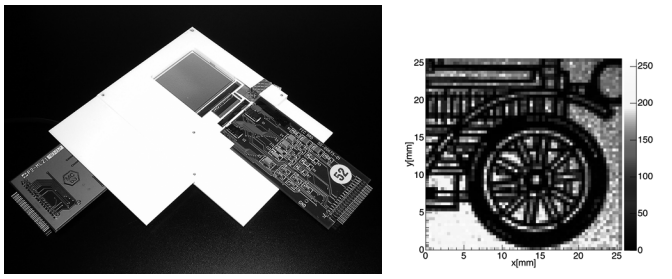

(a) (b)

Fig. 2. (a): The double-sided Si strip detector (DSSD). (b): A shadow picture obtained with the DSSD. 22 keV X-rays are used.

Fig. 3. The six layered DSSDs. The pitch between DSSD layers is 5.4 mm.

II. Setup

A. Stacked DSSDs

For the Compton scatterers, we use DSSDs with an area of 2.56 cm $\times$ 2.56 cm and a thickness of 300 μm. The strip pitch of the DSSD is 400 μm and 64 strips are implemented on each side.

The signals from the strips are processed by front-end-cards (FECs) on which two low noise analog ASICs, VA32TAs [18] are mounted. The strips on the p-side are connected directly to the input of the ASIC, while the strips of the n-side are connected via coupling capacitors. In order to obtain full depletion of the device, the n-side is biased with a voltage of 110 V. Since the spectral resolution of the p-side is better than that of the n-side, we have created spectra from the p-strips, and data from the n-strips are only used for positional information.

Fig. 2 shows a picture of the DSSD and a shadow image obtained with it. The shadow mask is a bookmark made of brass covered with gold, whose thickness is 0.8 mm. The image is created by collecting 22 keV X-rays from a ^{109}Cd source.

In order to increase the efficiency of Compton scattering, we stack six DSSDs. A picture of the six-layered DSSD is shown in Fig. 3. The gap between each DSSD layer is 5.4 mm.

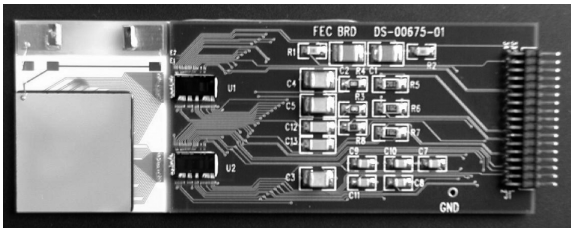

Fig. 4. The 8 $\times$ 8 CdTe pixel detector. The signal from each pixel is fed into VA32TAs on the FEC.

B. CdTe Pixel Detectors

We use 8 $\times$ 8 CdTe pixel detectors as absorbers in the Compton camera. The CdTe pixel detector is based on the Schottky CdTe diode device, utilizing indium as the anode and platinum as the cathode. By utilizing diode structure, we can obtain high energy resolution [10]–[12]. Fig. 4 shows a picture of the pixel detector. The detector has dimensions of 18.55 mm $\times$ 18.55 mm and a thickness of 500 μm. The indium side is used as a common electrode and is biased with a voltage of 400 V. The platinum side is divided into 8 by 8 pixels surrounded by a guard ring with a width of 1 mm. The pixel size is 2 mm $\times$ 2 mm, and the gap between the pixels is 50 μm. Each pixel is connected to a fanout board by using In/Au stud bump bonding technology [19]. The signal from each pixel is fed into the VA32TAs on-board the FEC. The VA32TA and FEC design are the same as that used in DSSD readout.

C. Compton Camera Setup

By combining the stacked DSSDs and three CdTe pixel detectors, we constructed a prototype Compton camera. A picture of the prototype is shown in Fig. 5. Two CdTe pixel detectors are placed underneath the DSSDs, and another detector is arranged on the side of the DSSDs.

A schematic diagram of the readout electronics is shown in Fig. 6. Signals from all detectors are fed into VA32TAs mounted on FECs. Fifteen FECs are connected to the interface card (IFC). The IFC provides bias currents/voltages for VA32TAs, and repeater functions for digital and analog circuit in the ASIC. The readout card (ROC) performs analog-to-digital conversions and readout sequence controls. A packet of data is constructed event by event in the ROC, and is sent to an acquisition computer via the serial data interface based on Space Wire network [20]. Detailed information on IFC and ROC is described in the paper of Mitani et al. [21]. In this prototype, the signals from the comparator outputs from the p-sides of six layered DSSDs and three CdTe pixel detectors are ORed to make trigger pulses. With each trigger, the pulse heights of all channels are acquired.

III. Data Analysis and Results

Using radio isotopes, we acquired data with the prototype to test the imaging and spectroscopy capabilities as a Compton camera. We placed the radio isotopes 350 mm above the surface

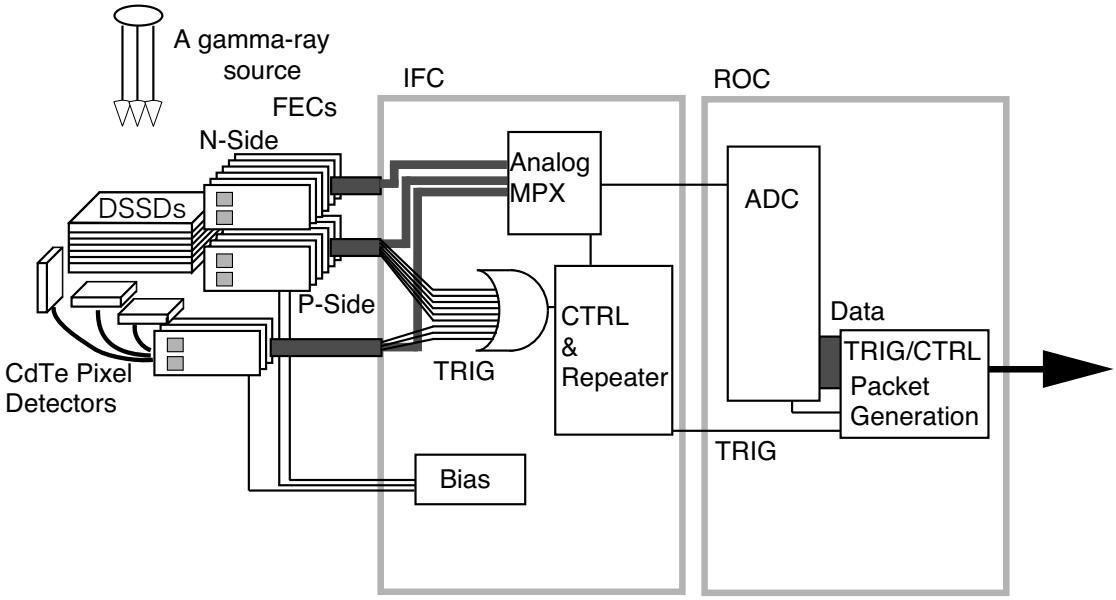

Fig. 6. The schematic diagram of the readout system.

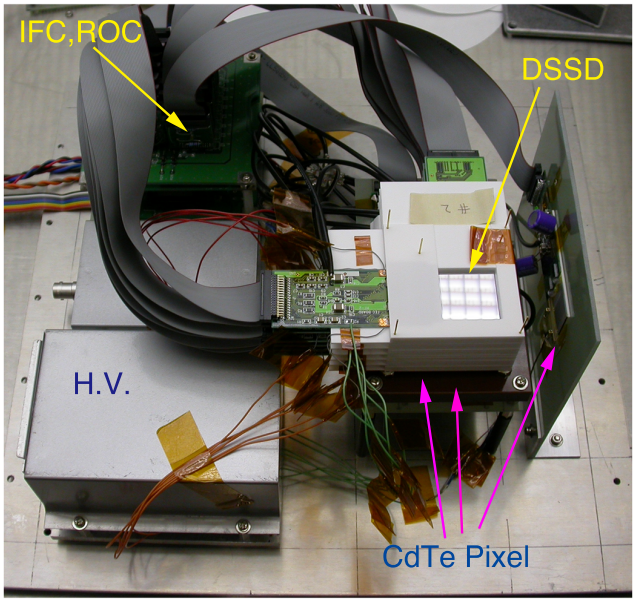

Fig. 5. The prototype of the DSSD/CdTe Compton Camera.

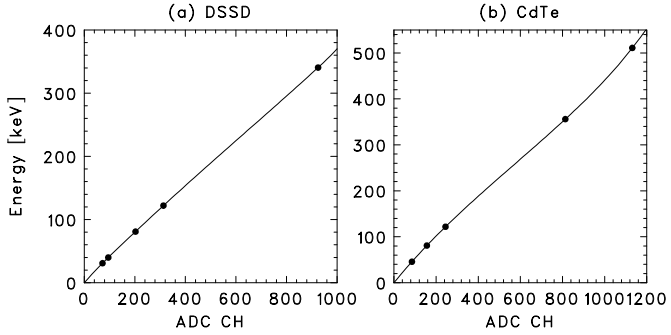

Fig. 7. The relation between ADC channel and energy is shown (a) for a strip of the DSSD and (b) for a pixel of the CdTe. The dots are obtained from positions of photo-absorption peaks. Additionally, for DSSDs, we also used the position of Compton edge of the 511 keV line. The lines show the third natural spline curves connecting all dots.

of the top DSSD. The strengths of the used isotopes are 1–3 MBq. Although there is no system to measure the dead time in our setup, the acquisition times of the following measurements are for several days in the real time. The DSSDs and the CdTe detectors were cooled to -5°C.

A. Single Hit Events

In order to reconstruct Compton events, relations between an ADC channel of a pulse height and an actual energy deposit must be obtained precisely. Therefore, we analyzed "single-hit events" and obtained photo-absorption peaks of gamma-ray lines from radio isotopes. The "single-hit" means that only one channel of the DSSDs or the CdTe pixel detectors has a pulse height above specified levels in the ADC unit. The levels correspond to about 15 keV and 25 keV for DSSDs and CdTe pixels, respectively.

Fig. 7 shows relations between ADC channel and energy for a DSSD strip and a CdTe pixel as typical examples. For DSSDs, in addition to the positions of photo-absorption peaks, positions of 511 keV Compton edges (341 keV) are used. As shown in the plots of Fig. 7, the energy deposits are not simply proportional to the ADC channels. Therefore, we adopted third neutral spline curves connecting all measured points for the calibration formula.

By using the relations obtained above, sum spectra of "single hit events" are created. Fig. 8 shows the spectra of DSSD ((a)) and CdTe pixel detector ((b)). The energy resolutions derived

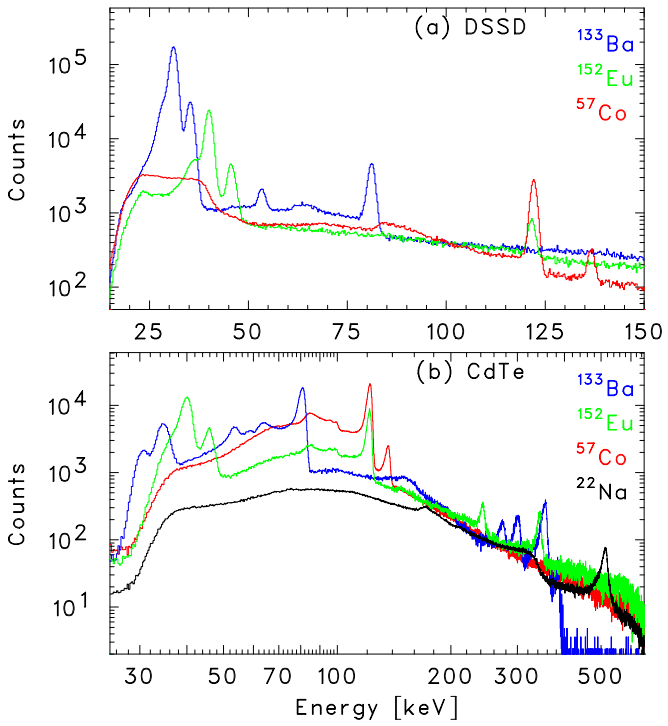

Fig. 8. The "single hit" spectra created from the DSSD events (a) and the CdTe events (b).

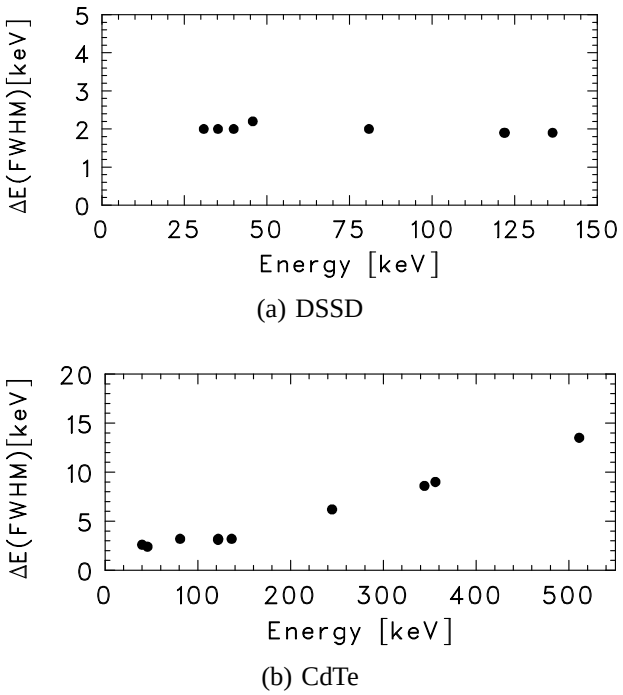

Fig. 9. The energy resolutions of (a) DSSD and (b) CdTe. For DSSD, the achieved energy resolution is about 2.0 keV regardless of energy. On the other hand, the energy resolution of CdTe is proportional to energy. $\Delta E/E$ is $\sim$ 2.5 %.

from these spectra are plotted in Fig. 9. The full-width-at-half-maximum (FWHM) of the DSSD is $\sim$ 2 keV regardless of the incident energy. Therefore, this energy resolution is attributable to the readout system. On the other hand, the FWHM of CdTe is proportional to the incident energy, and $\Delta E/E$ is about 2.5 %. This tendency means that the major contributor to the energy resolution is the charge loss due to low mobility and short lift-time of carriers in CdTe [25]. Though higher bias voltage should improve the energy resolution of CdTe, we kept the bias voltage of 400 V with the emphasis on stable operation.

B. Compton Reconstruction

For Compton reconstruction, data reduction is performed as follows. Firstly, "two-hit events", one hit in a DSSD and one hit in a CdTe, were selected from all the data. Here, one hit in a DSSD means that only one channel that is connected to a DSSD has a pulse hight above 8 keV, and one hit in a CdTe means that the only one channel that is connected to a CdTe detector has a pulse height above 20 keV. From each two-hit event, the information on the energy deposits detected in the DSSD ($E_{\rm Si}$) and in the CdTe detector ($E_{\rm CdTe}$) and their hit positions are obtained. Secondly, we calculate the incident gamma-ray energy (E_γ) and the scattering angle ($\theta_{\rm Comp}$). In the calculations, we assumed that incident gamma-rays are scattered in the DSSD and fully absorbed in the CdTe pixel detector. On this assumption,

$$E_\gamma = E_{\rm Si} + E_{\rm CdTe}, \tag{3}$$

and

$$\cos\theta_{\rm Comp} = 1 - \left(\frac{m_e c^2}{E_{\rm CdTe}} - \frac{m_e c^2}{E_{\rm Si} + E_{\rm CdTe}} \right). \tag{4}$$

From the calculated scattering angle and the two-hit positions, a Compton cone is drawn on the sky event by event. We projected the cone onto the plane at the distance of 350 mm, and obtained the image of the gamma-ray source.

Fig. 10 shows the Compton reconstructed images obtained with the prototype. A circle with a radius of 5 degree is drawn together with each image as reference. Fig. 10 (a) is the image of ^{57}Co 122 keV gammay-rays, by selecting events in which the sum of energy deposits at the DSSD and the CdTe pixel detector is within 118–128 keV. The image of ^{133}Ba events above 260 keV is shown in Fig. 10 (b). Fig. 10 (c) and (d) are images of ^{22}Na and ^{137}Cs, respectively. The selected energy regions are 500–520 keV and 650–675 keV, respectively. We note that the images are asymmetric because the arrangement of CdTe absorbers is not symmetric. Additionally, the "banana-shape" image of ^{57}Co 122 keV is caused by the fact that the scattering angle must be larger than 45° to deposit an energy larger than 8 keV at the DSSD, which is the energy threshold in this analysis.

In order to evaluate the angular resolution of our prototype Compton camera, we compare the calculated Compton-scattering angles ($\theta_{\rm Comp}$) with those defined by the location of gamma-ray source and hit positions ($\theta_{\rm Geom}$) (see Fig. 11). The difference between the two values reflects the angular resolution of the Compton camera. We examined the distri-

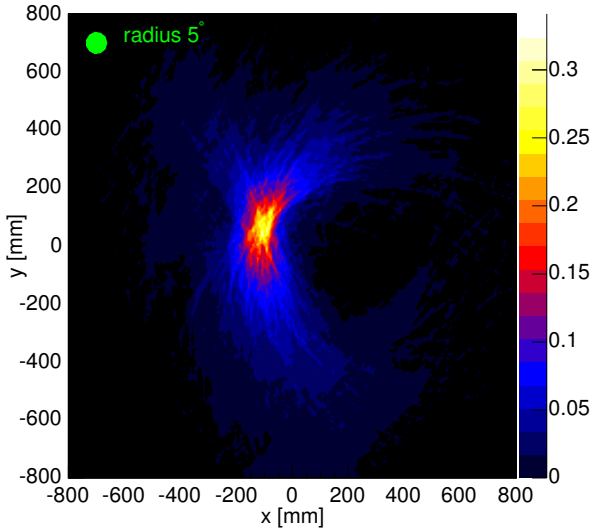

(a) ^{57}Co 122 keV

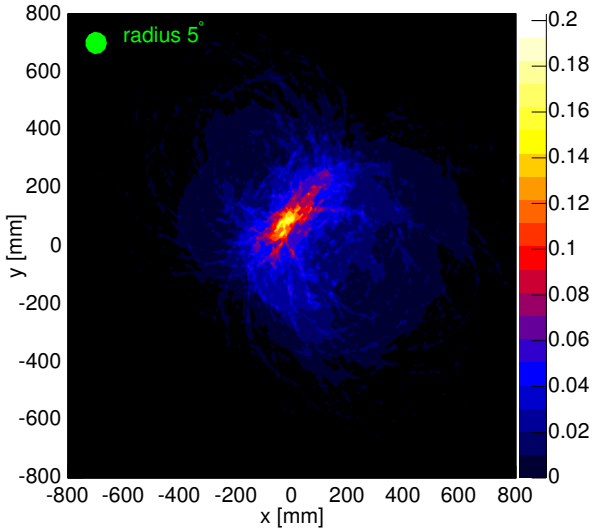

(b) ^{133}Ba 276, 303, 356, 384 keV

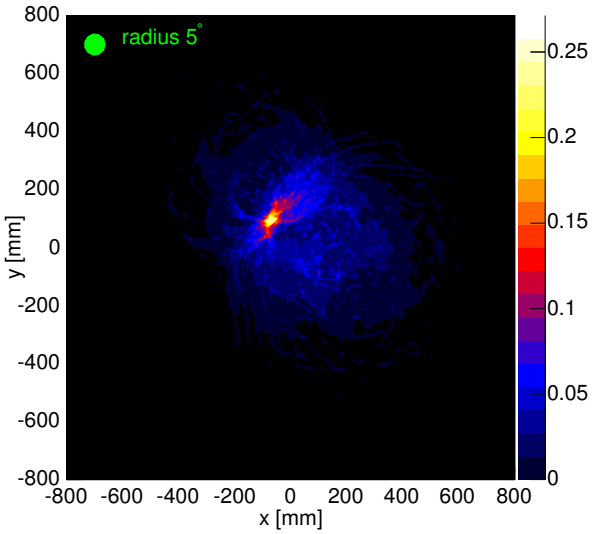

(c) ^{22}Na 511 keV

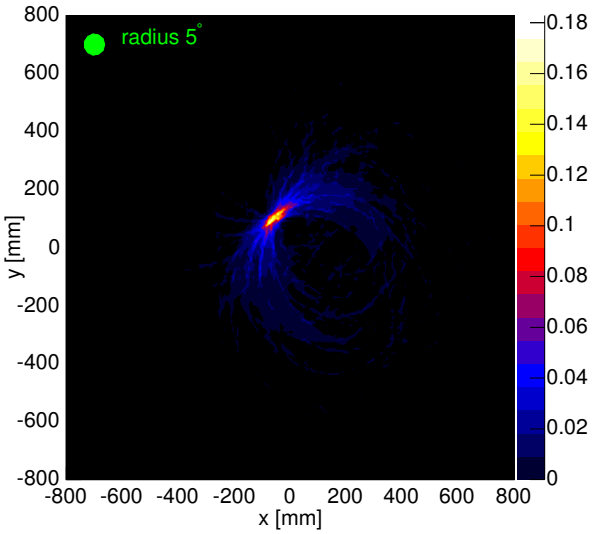

(d) ^{137}Cs 662 keV

Fig. 10. Compton reconstructed images of ^{57}Co, ^{133}Ba, ^{22}Na and ^{137}Cs. Circles with a radius of 5 degrees are drawn together with the images.

bution of $\theta_{\rm Comp} - \theta_{\rm Geom}$ for various peaks of ^{57}Co (122 keV and 136 keV), ^{133}Ba (356 keV), ^{22}Na (511 keV) and ^{137}Cs (662 keV). In Fig. 11, the distribution of $\theta_{\rm Comp} - \theta_{\rm Geom}$ for 511 keV events is shown as an example. The FWHM of these distributions, which is the angular resolution of the Compton camera, is plotted against the incident energy in Fig. 12. The angular resolution becomes better as the incident gamma-ray energy becomes higher.

We estimated the contributions of the position and the energy resolution of the DSSD and the CdTe detector. The contribution of the position resolution ($\Delta\theta_{\rm pos}$) is estimated by using the actual hit positions obtained from the experiment and the strip/pixel size of the DSSD and the CdTe detector. To estimate the contribution of the energy resolution ($\Delta\theta_{\rm ene}$), we used the Compton-scattering angles of actual events and smoothed them with the detector energy resolutions derived from "single-hit" events, which are $\Delta E \sim 2.0$ keV (FWHM) and $\Delta E/E \sim 2.5$ % (FWHM) for the DSSD and the CdTe pixel detector, respectively. In Fig. 12, the estimated values are plotted.

The other contributions to the angular resolution include the effect of "Doppler broadening". The Compton reconstruction is performed on the basis of eq. (3) and eq. (4), in which the target electrons are assumed to be free and at rest. In real detectors, however, target electrons are bound to their atomic nuclei with non-zero orbital momentum. The uncertainties of the bounding energy and the orbital momentum lead to the degradation of the angular resolution in Compton cameras. This effect is known as Doppler broadening [22]. In order to estimate the amount of Doppler broadening, we perform a Monte Carlo simulation using the Geant4 package [23]. As the code of Compton scattering including Doppler broadening, we use the package developed by R.M. Kippen [24]. In Fig. 12, the estimated values ($\Delta\theta_{\rm DB}$) from the simulation are also plotted. The effect of the Doppler broadening becomes smaller as the incident energy becomes higher, because the binding energy and momentum of electrons in materials become relatively small for gamma-ray photons with higher energies. In the same figure, the total values of $\Delta\theta_{\rm pos}$, $\Delta\theta_{\rm ene}$ and $\Delta\theta_{\rm DB}$:

$$\Delta\theta_{\rm total} = \sqrt{(\Delta\theta_{\rm pos})^2 + (\Delta\theta_{\rm ene})^2 + (\Delta\theta_{\rm DB})^2} \qquad (5)$$

are plotted together with the experimental data. The experimental values can be explained by the three contributions. In most cases, the angular resolution is limited by the effect of Doppler broadening, except that the contribution of position resolution is comparable to that of Doppler broadening in the higher energy region ($>$ 500 keV).

In order to obtain a clearer image, there is room for improvement in the arrangement of DSSD scatterers and CdTe absorbers. Because the Doppler broadening is restrained in the smaller scattering angles [7], [16], the arrangement that enables to pick up more events with a small scattering angle should contribute to make a clearer image. Since small angle scatters are associated with low energy scattering electrons, a lower energy threshold for DSSD becomes also important to pick up

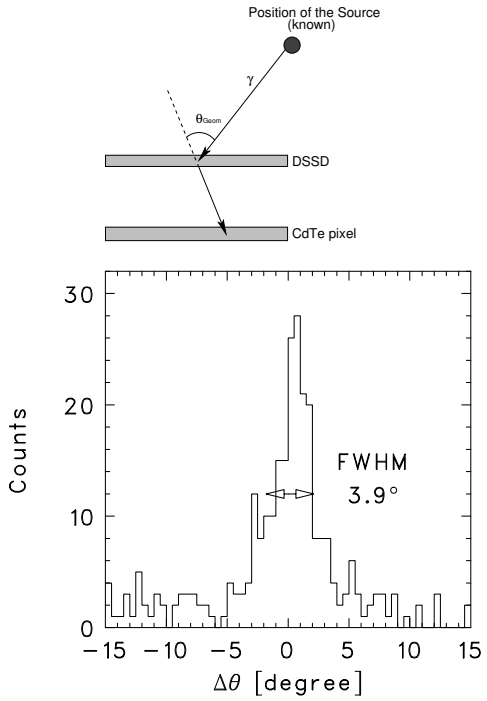

Fig. 11. Definition of $\theta_{\rm Geom}$ and distribution of $\theta_{\rm Comp} - \theta_{\rm Geom}$ for 511 keV events.

such events. Additionally, in order to obtain undistorted images, symmetric arrangement of CdTe absorber is indispensable.

The energy spectrum of a Compton camera can be obtained from the sum of energy deposits. The dashed line in Fig. 13 shows the spectrum obtained by simply summing the energies for all "two-hit events". In the spectrum, the four gamma-ray peaks (276 keV, 303 keV, 356 keV and 384 keV) from ^{133}Ba cannot be identified clearly. In a Compton camera, we can select events by using the Compton reconstructed image. The solid line spectrum drawn in Fig. 13 is made from the events satisfying the condition that the drawn Compton cone meets at the source position. The gamma-ray peaks are enhanced and four peaks are clearly resolved. The energy resolution is 9.1 keV (FWHM) at 356 keV.

Spectra of higher energy gamma-rays are shown in Fig. 14. The upper panel of Fig. 14 shows the spectrum of ^{22}Na, and the lower one shows the ^{137}Cs spectrum. The achieved energy resolutions are 14 keV (2.7 %) and 18 keV (2.7 %) at 511 keV and 662 keV, respectively. These values are consistent with the energy resolution of the DSSD ($\Delta E_{\rm Si}$(FWHM) $\sim$ 2.0 keV) and the CdTe pixel detector ($\Delta E_{\rm CdTE}/E \sim 2.5$ %), i.e. the energy resolution of this Compton camera is expressed as

$$\Delta E = \sqrt{(\Delta E_{\rm Si})^2 + (\Delta E_{\rm CdTe})^2}, \qquad (6)$$

In the case of this experiment, the energy resolution of the CdTe pixel detector limits the spectroscopic ability of this prototype. As discussed in § III-A, the energy resolution of the CdTe pixel detector is attributable to the charge collection efficiency. A higher bias voltage of $>$ 1000 V for 0.5 mm thickness is

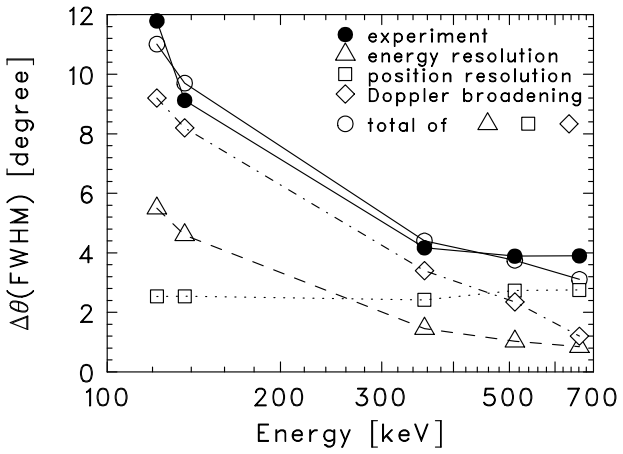

Fig. 12. Relation between incident gamma-ray energy and angular resolution. Filled circles show the experimental data. Open triangles, squares and diamonds are estimated contributions of detector energy resolution, detector position resolution and Doppler broadening, respectively. The total values of the three estimated values are plotted by open circles.

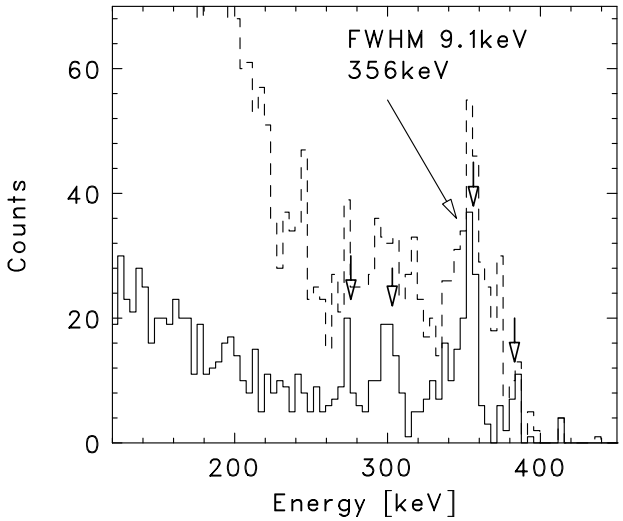

Fig. 13. Compton reconstructed spectra of ^{133}Ba. The dashed line shows the simple sum of two-hit events, while the solid line shows the sum of events identified to be emitted from the source by Compton reconstruction. The energy resolution is 9.1 keV (FWHM) at 356 keV.

required to achieve a $< 1\%$ energy resolution [25]. In order to enable such a high bias voltage, improvements in bump bonding and electrode formations are essential.

IV. Summary and Further Prospective

We have constructed a prototype Si/CdTe Compton camera, consisting of six-layered DSSDs and three 8×8 CdTe pixel detectors. By using this prototype, we have obtained Compton reconstructed images and spectra of gamma-rays from 122 keV to 662 keV. The achieved energy resolutions are 9.1 keV and 14 keV at 356 keV and 511 keV, respectively. The angular resolution is 3.9 degree (FWHM) for 511 keV gamma-ray photons.

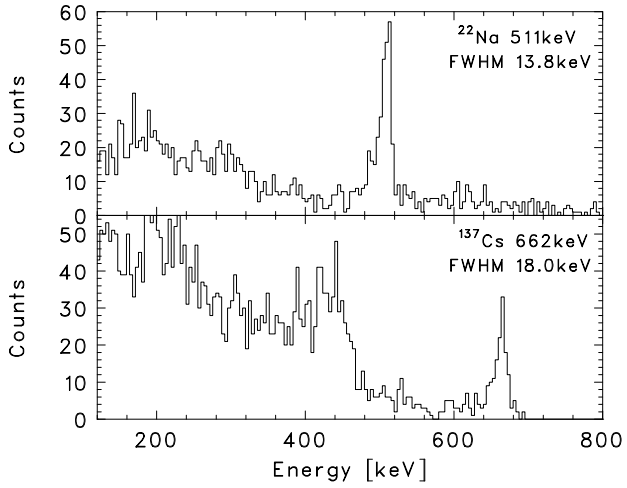

Fig. 14. Compton reconstructed spectra of ^{22}Na (upper) and ^{137}Cs (lower). The achieved energy resolutions are 13.8 keV and 18.0 keV for 511 keV and 662 keV gamma-rays, respectively.

In order to improve the quality of the Compton reconstruction image, the arrangement of DSSD scatterers and CdTe absorbers is important. Small scattering angles minimize the Doppler broadening effect, which limits the angular resolution of the prototype. In addition, a symmetric arrangement of CdTe absorbers is indispensable to obtain obtain undistorted images. On the other hand, for the higher energy resolution, it is essential to improve the energy resolution of CdTe absorbers. Based on the results, we are developing the next prototype, consisting of more DSSD layers and a symmetrical arrangement of CdTe absorbers. We are also addressing further improvements of CdTe detectors to achieve a high energy resolution.

Acknowledgment

The authors would like to thank C. Baluta for his critical reading of the manuscript.

References

[1] T. Takahashi, K. Makishima, Y. Fukazawa, M. Kokubun, K. Nakazawa, M. Nomachi, H. Tajima, M. Tashiro and Y. Terada, "Hard X-ray and γ-ray Detectors for the NEXT mission", *New Astronomy Reviews*, 48, pp. 269–273, 2004.

[2] T. Takahashi, A. Awaki, T. Dotani, Y. Fukazawa, K. Hayashida, T. Kamae, J. Kataoka, N. Kawai, S. Kitamoto, T. Kohmura, M. Kokubun, K. Koyama, K. Makishima, H. Matsumoto, E. Miyata, T. Murakami, K. Nakazawa, M. Nomachi, M. Ozaki, H. Tajima, M. Tashiro, T. Tamagawa, Y. Terada, H. Tsunemi, T. Tsuru, K. Yamaoka, D. Yonetoku, and A. Yoshida, "Wide band X-ray Imager (WXI) and Soft Gamma-ray Detector (SGD) for the NeXT Mission", *Proc. SPIE*, 5488, pp. 549–560, 2004.

[3] T. Takahashi, K. Nakazawa, T. Kamae, H. Tajima, Y. Fukazawa, M. Nomachi and M. Kokubun, "High resolution CdTe detectors for the next generation multi-Compton gamma-ray telescope", *Proc. SPIE*, 4851, pp. 1228–1235, 2003.

[4] G. Kanbach, R. Andritschke, F. Schopper, V. Schönfelder, A. Zoglauer, P.F. Bloser, S.D. Hunter, J.A. Ryan, M. McConnell, V. Reglero, G. DiCocco and J. Knödlseder, "The MEGA project", *New Astronomy Reviews*, 48, pp. 275–280, 2004.

[5] J.D. Kurfess, W.N. Johnson, R.A. Kroeger, B.F. Phlips and E.A. Wulf, "Development and applications of position-sensitive solid-state gamma ray detectors", *Nucl. Instrum. Methods*, A505, pp. 256–264, 2003.

[6] T. J. O'Neill, D. Bhattacharya, M. Polsen, A.D. Zych, J. Samimi and A. Akyuz, "Development of the TIGRE Compton telescope for intermediate-energy gamma-ray astronomy", *IEEE Trans. Nucl. Sci.*, vol. 50, pp. 251–257, 2003.

[7] Y.F. Du, Z. He, G.F. Knoll, D.K. Wehe and W. Li, "Evaluation of a Compton scattering camera using 3-D position sensitive CdZnTe detectors", *Nucl. Instrum. Methods*, A457, pp. 203–211, 2001.

[8] T. Kamae, R. Enomoto and N. Hanada, "A new method to measure energy, direction, ans polarization of gamma rays", *Nucl. Instrum. Methods*, A260, pp. 254–257, 1987.

[9] F. Lei, A.J. Dean and G.L. Hills, "Compton polarimetry in gamma-ray astronomy", *Space Science Reviews*, 82, pp. 309–388, 1997.

[10] T. Takahashi, T. Mitani, Y. Kobayashi, M. Kouda, G. Sato, S. Watanabe, K. Nakazawa, Y. Okada, M. Funaki, R. Ohno and K. Mori, "High Resolution Schottky CdTe Detector," *IEEE Trans. Nucl. Sci.*, vol. 49, pp. 1297–1303, 2002.

[11] T. Tanaka, Y. Kobayashi, T. Mitani, K. Nakazawa, K. Oonuki, G. Sato, T. Takahashi and S. Watanabe, "Recent achievements of the high resolution Schottky CdTe diode for γ-ray detectors", *New Astronomy Reviews*, 48, pp. 309–313, 2004.

[12] K. Nakazawa, K. Oonuki, T. Tanaka, Y. Kobayashi, K. Tamura, T. Mitani, G. Sato, S. Watanabe, T. Takahashi, R. Ohno, A. Kitajima, Y. Kuroda and M. Onishi, "Improvement of the CdTe Diode Detectors using a Guard-ring Electrode", *IEEE Trans. Nucl. Sci.*, vol. 51, pp. 1881–1885, 2004.

[13] Y. Fukazawa, T. Nakamoto, N. Sawamoto, S. Uno, T. Ohsugi, H. Tajima, T. Takahashi, T. Mitani, T. Tanaka and K. Nakazawa, "Low-noise Double-sided Silicon Strip Detector for Soft Gamma-ray Compton Camera", *Proc. SPIE*, 5501, 2004.

[14] H. Tajima, T. Kamae, S. Uno, T. Nakamoto, Y. Fukazawa, T. Mitani, T. Takahashi, K. Nakazawa, Y. Okada and M. Nomachi, "Low Noise Double-Sided Silicon Strip Detector for Multiple-Compton Gamma-ray Telescope", *Proc. SPIE*, 4851, pp. 875–884, 2003.

[15] R. Ribberfors, "Relationship of the relativistic Compton cross section to the momentum distribution of bound electron states", *Phys. Rev. B*, vol. 12, pp. 2067–2073, 1975.

[16] T. Tanaka, T. Mitani, S. Watanabe, K. Nakazawa, K. Oonuki, G. Sato, T. Takahashi, K. Tamura, H. Tajima, H. Nakamura, M. Nomachi, T. Nakamoto and Y. Fukazawa, "Development of a Si/CdTe semiconductor Compton telescope", *Proc. SPIE*, 5501, pp. 229–240, 2004.

[17] T. Mitani, T. Tanaka, K. Nakazawa, T. Takahashi, H. Tajima, H. Nakamura, M. Nomachi, T. Nakamoto and Y. Fukazawa, "A Prototype of Si/CdTe Compton Camera and the Polarization Measurement", *IEEE Trans. Nucl. Sci.*, vol. 51, pp. 2432–2437, 2004.

[18] H. Tajima, T. Nakamoto, T. Tanaka, S. Uno, T. Mitani, E do Couto e Silva, Y. Fukazawa, T. Kamae, G. Madejski, D. Marlow, K. Nakazawa, M. Nomachi, Y. Okada and T. Takahashi, "Performance of a Low Noise Front-end ASIC for Si/CdTe Detectors in Compton Gamma-ray Telescope", *IEEE Trans. Nucl. Sci.*, vol. 51, pp. 842–847, 2004.

[19] T. Takahashi, S. Watanabe, M. Kouda, G. Sato, S. Kubo, Y. Kuroda, M. Onishi and R. Ohno, "High Resolution CdTe Detector and Applications to Imaging Devices," *IEEE Trans. Nucl. Sci.* vol. 48, No.3, pp. 281–291, 2001.

[20] M. Nomachi, S. Ishii, Y. Kuroda, H. Nakamura, T. Sugimoto and T. Takahashi, "A Data Readout System with High-Speed Serial Data Link for Balloonborne X-ray Detectors", *IEEE Trans. Nucl. Sci.*, submitted in 2004

[21] T. Mitani, H. Nakamura, S. Uno, T. Takahashi, K. Nakazawa, S. Watanabe, H. Tajima, M. Nomachi, Y. Fukazawa, S. Kubo, Y. Kuroda, M. Onishi and R. Ohno, "Large area Gamma-ray Imaging Detector Based on High Resolution CdTe Diode", *IEEE Trans. Nucl. Sci.*, vol. 50, pp. 1048–1052, 2003.

[22] A. Zoglauer and G. Kanbach, "Doppler broadening as a lower limit to the angular resolution of next generation Compton telescopes", *Proc SPIE*, 4851, pp. 1302–1309, 2003.

[23] S. Agostinelli et al., "GEANT4– a simulation toolkit", *Nucl. Instrum. Methods*, A506, pp. 250–303, 2003.

[24] R.M. Kippen, "The GEANT low energy Compton scattering (GLECS) package for use in simulating advanced Compton telescopes", *New Astronomy Reviews*, 48, pp. 221–225, 2004.

[25] T. Takahashi and S. Watanabe, "Recent Progress in CdTe and CdZnTe Detector," *IEEE Trans. Nucl. Sci.*, vol. 48, No. 4, pp. 950-959, 2001.